

## Structural evolution of $\text{Bi}_2\text{O}_3$ prepared by thermal oxidation of bismuth nano-particles

A. J. Salazar-Pérez, M. A. Camacho-López\*, R. A. Morales-Luckie, V. Sánchez-Mendieta  
*Facultad de Química-Universidad Autónoma del Estado de México*  
*Paseo Colón y Tolloca, C.P. 50130, Toluca, México*

F. Ureña-Núñez  
*Instituto Nacional de Investigaciones Nucleares*  
*A.P. 18-1027, Col. Escandón, Delegación Miguel Hidalgo, C.P. 11801, México, D.F.*

J. Arenas-Alatorre  
*Instituto de Física-Universidad Nacional Autónoma de México*  
*Apdo. Postal 20-364 México 01000 D.F.*  
 (Recibido: 9 de junio de 2005; Aceptado: 13 de agosto de 2005)

Bismuth nano-sized particles were prepared by the chemical reduction method. These particles were characterized by HR-TEM, X-Ray Diffraction and Micro-Raman Spectroscopy. In order to obtain bismuth oxide, the as-obtained bismuth nano-particles were thermally treated in air at various temperatures in the range 100-750 °C during 30 min. The thermally treated samples were studied by Micro-Raman Spectroscopy. Additionally, information on the chemical composition and morphology was obtained by Energy Dispersive Spectroscopy and Scanning Electron Microscopy, respectively. Results show that bismuth nano-particles were oxidized at 100 °C and transformed into three of the five phases of  $\text{Bi}_2\text{O}_3$  reported in literature; the obtained phase depends on the annealing temperature. The  $\beta\text{-Bi}_2\text{O}_3$  phase was obtained for 200-300 °C,  $\alpha\text{-Bi}_2\text{O}_3$  for 400-600 °C and finally  $\gamma\text{-Bi}_2\text{O}_3$  for 700-750 °C.

*Keywords:* Bismuth oxide; Thermal oxidation; Micro-Raman spectroscopy

### 1. Introduction

Bismuth is a semimetal with a rhombohedral structure. The synthesis of bismuth nanoparticles has been recently reported by using a chemical method [1]. Bismuth oxide can be obtained from bismuth through an oxidation process in air or oxygen. C. C. Huang et al have reported the study of the oxidation process in electrodeposited bismuth films [2]. The authors have found that the crystalline phase formed during the oxidation process depends on the orientation of the as-electrodeposited Bi film.

There exists five polymorphs of bismuth oxide ( $\text{Bi}_2\text{O}_3$ ) named:  $\alpha\text{-Bi}_2\text{O}_3$  (monoclinic),  $\beta\text{-Bi}_2\text{O}_3$  (tetragonal),  $\gamma\text{-Bi}_2\text{O}_3$  (BCC),  $\delta\text{-Bi}_2\text{O}_3$  (Cubic),  $\epsilon\text{-Bi}_2\text{O}_3$  (triclinic).  $\alpha\text{-Bi}_2\text{O}_3$  transforms into  $\delta\text{-Bi}_2\text{O}_3$  at 729 °C [3-5]. The cooling of the  $\delta\text{-Bi}_2\text{O}_3$  phase gives rise to the  $\beta\text{-Bi}_2\text{O}_3$  at 650 °C or the  $\gamma\text{-Bi}_2\text{O}_3$  at 639 °C.  $\beta\text{-Bi}_2\text{O}_3$  and  $\gamma\text{-Bi}_2\text{O}_3$  are metastable phases that can be stabilized to exist at room temperature by doping with impurities such as niobium or tantalum. N. Cornei et al. have recently reported the synthesis of a new phase named  $\epsilon\text{-Bi}_2\text{O}_3$  by using the so called hydrothermal method [5]. The authors found that this polymorph is an ionic insulator in contrast to  $\beta$ -,  $\gamma$ -,  $\delta\text{-Bi}_2\text{O}_3$  (ionic conductors).

Raman spectroscopy is a powerful tool to identify different polymorphs of metal oxides. For instance, the polymorphs of  $\text{TiO}_2$ : anatase, brookite and rutile and the ones of  $\text{MoO}_3$ :  $\alpha$ -,  $\beta$ - and  $\beta'$ -  $\text{MoO}_3$  have been characterized by using the Raman technique [6-8]. S. N. Narang et al. have reported Raman data for the  $\alpha\text{-Bi}_2\text{O}_3$

phase. F. Hardcastle and I. E. Washs have reported the  $\beta$ - and  $\delta\text{-Bi}_2\text{O}_3$  Raman spectra for niobia and tantalum stabilized bismuth oxide. Also Raman spectra of sillenite structures have been reported by several authors [9-11]. It is well known that  $\alpha\text{-Bi}_2\text{O}_3$  and  $\beta\text{-Bi}_2\text{O}_3$  have Raman features in the 50-600  $\text{cm}^{-1}$  range while  $\gamma\text{-Bi}_2\text{O}_3$  and  $\delta\text{-Bi}_2\text{O}_3$  in the 50-900  $\text{cm}^{-1}$ . To the best of our knowledge there not exists Raman data for the  $\epsilon\text{-Bi}_2\text{O}_3$  (triclinic) phase reported yet.

The aim of this work was to characterize the structural and morphological changes that occur to bismuth nanoparticles upon thermal oxidation. The crystalline phases of bismuth oxide were studied and analyzed by micro-Raman spectroscopy. We identified three out of the five phases that are already well known for the  $\text{Bi}_2\text{O}_3$ .

### 2. Experimental

#### 2.1 Synthesis of bismuth nanoparticles

$\text{Bi}(\text{NO}_3)_3$  and sodium borohydride were used to synthesize bismuth nanoparticles by the chemical reduction method. A typical procedure carried out in aerobic condition, room temperature and ambient pressure involves the preparation of a pH free solution of salt of Bi (1Lt) at a concentration of  $1 \times 10^{-2}$  M ( 3.956 g.) and a reductor (100 ml) at a pH=11 at concentration  $1.5 \times 10^{-2}$  M (0.567 g) poured instantaneously and followed by cooling of both

\*marcel@uaemex.mx

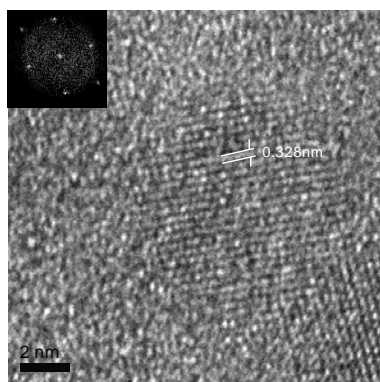


**Figure 1.** HR-TEM micrograph of the as-synthesized Bismuth nanoparticles. The inset Fast Fourier Transform obtained from HR-TEM.

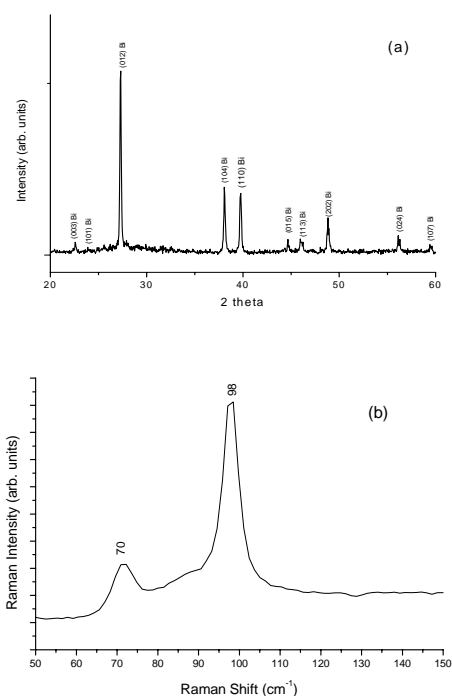


**Figure 2.** (a) XRD pattern and (b) Micro-Raman spectrum of the as-synthesized bismuth particles.

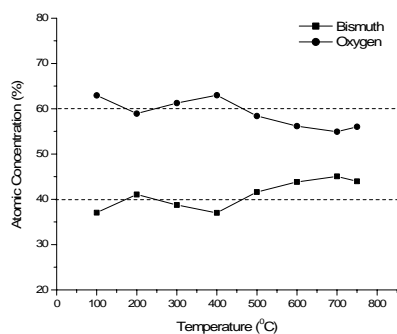


**Figure 3.** Bismuth and oxygen content in the thermal treated bismuth particles as a function of temperature.

solutions at 5° C. The process is started by the addition of the whole amount of reductor solution at once in order to avoid the nucleation effect and therefore the growth of particles; at the beginning of the reaction the solution acquires a dark color due to the precipitation of particles. Afterwards, the products of the reaction are filtered several times using a Buchner funnel and deionized water to remove the undesired ions, and subsequently washing with acetone (100 ml aprox.) to eliminate water.

## 2.2 Oxidation process

The oxidation process of the bismuth nanoparticles was carried out by placing 1.5 gr of the as-synthesized bismuth powder on a silicon wafer. Thermal treatments at 100, 200, 300, 400, 500, 600, 700 and 750 °C for 30 minutes each was carried out in a tubular oven (Minimite, Sola Basic). For each temperature a whole thermal cycle consisted of: 20 °C/min heating, the particular constant temperature (30 min) and 10 °C/min cooling.

## 2.3 Sample characterization

The as-synthesized bismuth powders were characterized by High Resolution Transmission Electron Microscopy (HR-TEM) using a system JEOL JEM-2010F, X-Ray Diffraction (XRD) and Micro-Raman Spectroscopy (MRS). XRD patterns were obtained with a diffractometer Siemens D-5000. The thermal treated bismuth samples were characterized by MRS, Scanning Electron Microscopy (SEM) and Energy Dispersive Spectroscopy (EDS). All the Raman measurements were done with a Micro-Raman system Jobin-Yvon-Horiba (HR-800) equipped with a Microscope Olympus (BX-41) and a CCD as detector. A He-Ne laser (emission at 632.8 nm) at a power level of 60 μW was used as the excitation source. EDS and SEM measurements were performed using a scanning electron microscope JEOL, JSM 5900 LV.

## 3. Results

### 3.1 Bismuth nano-particles

Figure 1 shows a HR-TEM micrograph of the as-synthesized bismuth particles. The presence of a nano-sized particle of about 10nm can be seen. The interplanar distance measured was 0.328nm that corresponds to planes oriented in the direction (012) of rhombohedral bismuth.

The Fast Fourier Transform (FFT) technique (inset in figure 1) allowed us to measure the interplanar distance  $d_{hkl} = 0.2346\text{nm}$  corresponding to the planes (104) of the rhombohedral phase according to the JCPDS-ICDD 44-1246 card.

Figure 2 shows results of XRD and MRS for the as-synthesized bismuth nano-particles. The diffraction pattern (Figure 2a) presents peaks corresponding to reflexion planes of the rhombohedral structure of metallic bismuth. The Micro-Raman spectrum (Figure 2b) shows the

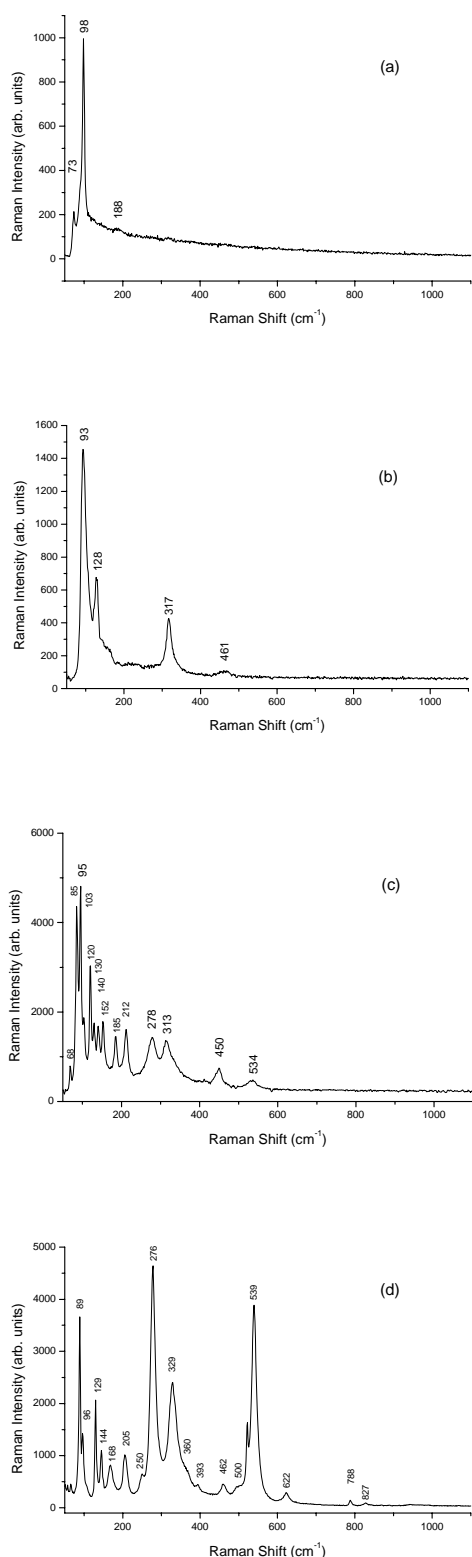


**Figure 4.** Raman spectra of thermal treated bismuth particles at (a) 100, (b) 300, (c) 600 and (d) 750 °C.

vibrational features that are located between 50 and 150  $\text{cm}^{-1}$  which is the region where bismuth has Raman activity.

According to what is reported in the literature, the two peaks at 70 and 98  $\text{cm}^{-1}$  are indicative of the rhombohedral bismuth structure. In this way, our Raman results confirm the ones that were obtained by XRD.

### 3.2 Bismuth Oxide

Figure 3 shows the EDS results obtained for the thermal treated bismuth samples. The EDS results are the average of 3 measurements done at different locations on the sample. One can see that for a temperature of 100 °C the material is constituted by bismuth and oxygen. For temperatures between 100-400 °C, the atomic concentration of bismuth and oxygen is closer to that corresponding to  $\text{Bi}_2\text{O}_3$ .

When the thermal treatment temperature is in the range of 500-750 °C, it is clear that the oxygen content diminishes. This indicates that the obtained bismuth oxide is oxygen deficient.

A total of five phases of  $\text{Bi}_2\text{O}_3$  have been reported in the literature. Table 1 lists and compares the Raman frequencies found through our work to the corresponding three phases of bismuth oxide previously reported in the literature. As it can be immediately seen our results are in good agreement to those reported in the literature.

Figure 4 (a-d) shows Micro-Raman spectra of the oxidized bismuth particles as it was described in section 2.2. The Micro-Raman spectra were all taken in the range 50 to 1100  $\text{cm}^{-1}$ . The spectrum 4a corresponds to the sample treated at 100 °C. This spectrum is constituted by only the two peaks found for bismuth (figure 2b) indicating that the rhombohedral structure predominates at this temperature. However, when the temperature is increased up to 200 °C the Raman changes are evident. For 200 and 300 °C the Raman features were very similar, so the Raman spectrum of the sample annealed at 200 °C is not presented here. Spectrum 4b corresponds to the sample annealed at 300 °C. In this case, new peaks centered at 130, 317 and 461  $\text{cm}^{-1}$  appear which can be attributed to the  $\beta\text{-Bi}_2\text{O}_3$  (tetragonal) phase. This indicates that the thermal treatment of bismuth at this temperature induced two effects: an oxidation followed by a structural transformation from the rhombohedral (Bi) structure to the tetragonal ( $\beta\text{-Bi}_2\text{O}_3$ ) one. For the samples treated at 400, 500 and 600 °C no significant Raman changes in the spectra were found. For this reason only the Raman spectrum corresponding to the sample treated at 600 °C is presented.

The Raman spectrum 4c presents new Raman peaks that can be attributed to the  $\alpha\text{-Bi}_2\text{O}_3$  (monoclinic) phase. The intensity and frequency of the Raman peaks corresponding to the samples treated at 700 and 750 °C are similar indicating that the achieved crystalline phase at these two temperatures is the same. The spectrum 4d corresponds to the sample annealed at 750 °C; the set of Raman peaks in this case can be attributed to the  $\gamma\text{-Bi}_2\text{O}_3$  phase (Table 1).

**Table 1.** Raman frequencies for some Bi<sub>2</sub>O<sub>3</sub> phases.

$\beta$ -Bi <sub>2</sub> O <sub>3</sub> <sup>a</sup>	Our work 200-300 (°C)	$\alpha$ -Bi <sub>2</sub> O <sub>3</sub> <sup>b</sup>	Our work 400-600 (°C)	$\gamma$ -Bi <sub>2</sub> O <sub>3</sub> <sup>c</sup> Bi <sub>12</sub> SiO <sub>20</sub>	Our work 700-750 (°C)
				841	
				828	827
				789	788
				623	622
		513	534	540	539
462	461	467		498	500
		448	450	461	462
		438			
		410			
311	317	340			393
		314	313	370	369
				328	329
		281	278	278	276
		210	212	250	250
				208	205
124	128	184	185	166	168
		156		145	144
		151	152	130	129
		146			
		138	140		
			130		
		118	120		
		101	103		
	93	91	95	98.8	96
		82	85	89.2	89
		65	68		65
		57		58.0	55
				53.5	
				50.6	
				46.1	
				44.4	

<sup>a</sup>F. D. Hardcastle et al.<sup>b</sup>S. N. Narang et al.<sup>c</sup>S. Venugopalan and A. K. Ramdas

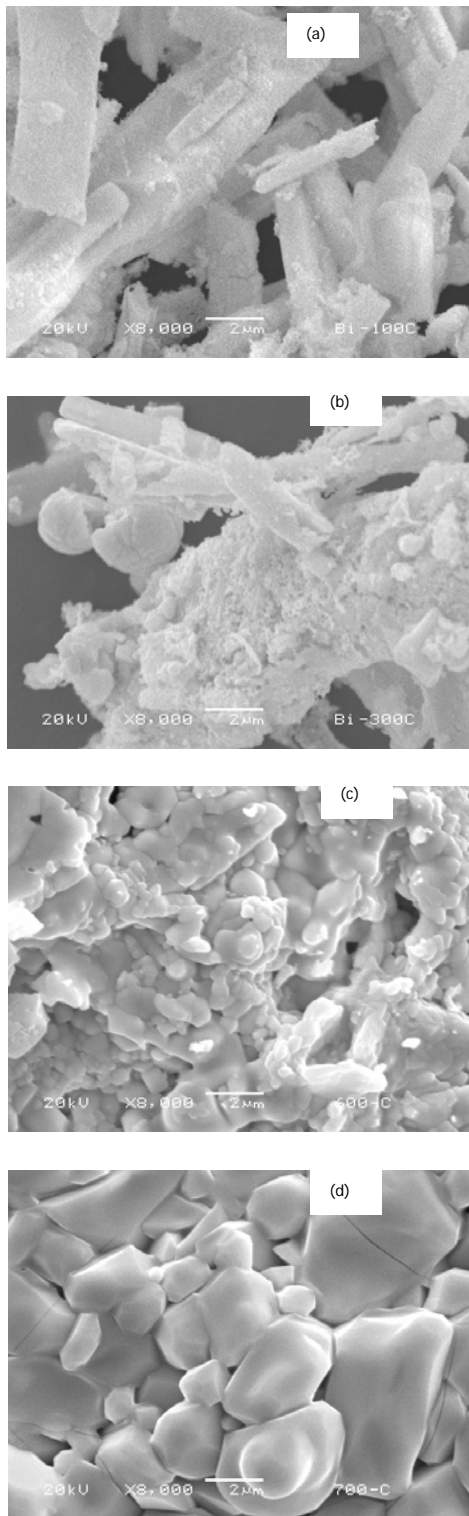
This phase is isostructural with the so-called sillenite (Bi<sub>12</sub>SiO<sub>20</sub>) structure. The Raman spectrum for Bi<sub>12</sub>SiO<sub>20</sub> single crystals has been reported by some authors [9-11].

Figure 5(a-d) shows SEM images of the bismuth samples treated at 100, 300, 600 and 750 °C, respectively. In all cases the micrographs have the same amplification.

Figure 5a exhibits a morphology constituted by filaments type needles; however these needles begin to form agglomerates when the temperature within the thermal treatment increases up to 300 °C (figure 5b). At 600 °C (figure 5c) the morphology of the bismuth is composed by amorphous particles covered by small granules. After a thermal treatment at 750 °C the morphology of the bismuth has changed from filaments type needles to micro-spheroid particles as can be clearly seen in figure 5d.

#### 4 Conclusions

In this work we report the structural evolution of nano-sized bismuth upon thermal oxidation in air. Micro-Raman spectroscopy was used ex-situ to monitor the structural changes that occur through the oxidation process. We have found that the starting material is oxidized at 200 °C. Phase transitions of Bi<sub>2</sub>O<sub>3</sub> were clearly identified for the temperature range 200-750 °C:  $\beta$ -Bi<sub>2</sub>O<sub>3</sub> (200-300 °C) to  $\alpha$ -Bi<sub>2</sub>O<sub>3</sub> (400-600 °C) to  $\gamma$ -Bi<sub>2</sub>O<sub>3</sub> (700-750 °C). Finally, we found that the microcrystal morphology was different for the three formed phases.



**Figure 5.** SEM micrographs of thermal treated bismuth particles at (a) 100, (b) 300, (c) 600 and (d) 750 °C.

## Acknowledgments

This work was financially supported through the projects: PROMEP103.5/04/1352 and UAEM 1950/2004B

## References

- [1] Wang, Y. W., Hee Hong Byung and S. Kim Kwang, *J. Phys. Chem.* 109, 7067 (2005).
- [2] C. C. Huang, T. Y. Wen, K. Z. Fung, *Materials Research Bulletin* 41, 110(2006).
- [3] Narang S. N., Patel N. D. , Kartha V. B., *Journal of Molecular Structure* 327, 221 (1994).
- [4] Hardcastle Franklin D. and Wachs Israel E., *Journal of Solid State Chemistry*, 97, 319 (1992).
- [5] N. Cornei, N. Tancet, F. Abraham, O. Mentré, *Inorganic Chemistry* (2006).
- [6] G. A. Tompsett, G. A. Bowmaker, R. P. Cooney, J. B. Metson, K. A. Rodgers and J. M. Seakins, *J. Raman Spectroscopy* 26, 57(1985).
- [7] I.R. Beattie, T.R. Gilson, *J. Chem. Soc. A* 2322 (1969).
- [8] E.M. McCarron III, *J. Chem. Soc. Chem. Commun.* 336 (1986).
- [9] G.A. Nazri, C. Julien, *Solid State Ionics*, 53 376 (1992).
- [10] S. Venugopalan, A. K. Ramdas, *Physical Review B* 5, 4065 (1972).
- [11] L. Escobar-Alarcón, E. Haro-Poniatowski, M. Fernández-Guati, A. Perea, C. N. Afonso, T. Falcón, *Appl. Phys. A*, 69, 949 (1999).
- [12] B. Mihailova, M. Gospodinov, L. Konstantinov, *J. Phys. Chem. Solids* 60, 1821 (1999).